SWIPT in FA-enabled Cellular Networks: A Stochastic Geometry Copula-based Approach

Christodoulos Skouroumounis and Ioannis Krikidis
IRIDA Research Centre for Communication Technologies,
Department of Electrical and Computer Engineering, University of Cyprus, Cyprus
Email: {cskour03, krikidis}@ucy.ac.cy

***Abstract*—By utilizing the combination of two powerful tools i.e., stochastic geometry (SG) and copula theory (CT), in this paper, we assess the performance of fluid-based reconfigurable antenna (FA)-enabled user equipments (UEs) in the context of simultaneous wireless information and power transfer (SWIPT) networks. Particularly, by using CT tools, we initially derive a closed-form expression for the cumulative distribution function of the observed signal-to-interference ratio (SIR) under correlated Nakagami-μ fading channels by exploiting a well-investigated Archimedean copula, namely the Frank copula. According to the CT-based approach, a SG-based framework is presented to assess the SWIPT performance of FA-enabled UEs, that are equipped with a power splitting scheme to simultaneously extract information and harvest energy from the port with the strongest SIR. Our results reveal that FA-enabled SWIPT systems experience an improved information decoding performance of around 30% with a slight reduction in energy harvest performance of around 6% compared to conventional fixed-positioned antennas systems.**

***Index Terms*—Fluid antenna, SWIPT, port selection, stochastic geometry.**

I. Introduction

The introduction of sixth-generation (6G) networks and the revolutionary concept of the massive Internet of Things (mIoT) have sparked a substantial surge in the demand for ultra-reliable connectivity, while simultaneously enhancing the longevity of energy-constrained networks [1]. Towards fulfilling this demand, extensive research has been conducted on multi-user/multi-antenna communication technologies. These technologies, commonly referred to as multiple-input multiple-output (MIMO), aim to enhance spectral and energy efficiency through the utilization of spatial multiplexing techniques [2].

Nevertheless, to ensure full diversity gain in MIMO systems, antennas must be positioned at a minimum separation of half the radiation wavelength, which poses challenges for mobile devices with physical space limitations [3]. Additionally, conventional MIMO systems with fixed-positioned antennas (FPAs) have limited utilization of the available degrees of freedom in the continuous spatial domain, impacting spatial diversity and multiplexing performance optimization [4]. To overcome these inherent constraints, a novel approach known as fluid-based reconfigurable antennas (FAs) has emerged. Different from conventional FPAs, FAs can be programmably and controllably moved to different locations (ports) within a confined region. This unique capability of FAs allows the fully exploitation of the spatial degrees-of-freedom for improving the wireless channel condition. Thus, the concept of FA-enabled communications has garnered considerable attention from both the research community and industry, resulting in their investigation across a diverse range of point-to-point [4]–[6] and large-scale [7], [8] communication scenarios. Regarding characterizing the fading channel correlation between the FA ports, the majority of existing works applied either the traditional statistical methods or asymptotic formulations, leading to an escalated analytical complexity. The concept of copula theory (CT), on the other hand, is a promising low-complexity alternative approach that has been overlooked. Recently, the concept of CT has gained significant interest in the performance analysis of different wireless communication systems. In the context of FA-enabled networks, the authors in [9] focus on investigating the outage and delay performance of single-user communication scenarios, by utilizing CT tools.

Achieving energy self-sustainability of battery-less devices/applications, thereby prolonging the lifetime of mIoT systems, is another significant challenge faced by the next-generation networks [10]. This demand led to the introduction of simultaneous wireless information and power transfer (SWIPT) systems, where UEs are able to extract both information and energy from radio-frequency (RF) signals. In the past, the possibility of implementing SWIPT-enabled wireless networks was considered infeasible, due to the inherent difficulty of receivers to decode information and harvest energy at the same time. Fortunately, the concept of SWIPT becomes feasible by partitioning the received RF signal into two distinct parts: one intended for information decoding (ID) and the other for energy harvesting (EH). This can be achieved by orthogonalizing the resources in the time, power, or space domain [10]. Throughout the literature, the potential benefits of SWIPT have been widely acknowledged and the performance of SWIPT-enabled communications has been extensively investigated [11], [12]. However, the co-design of SWIPT and FA technologies, as well as the performance evaluation in large-scale cellular networks by employing stochastic geometry (SG) and CT tools has been disregarded.

Motivated by this, in this paper, we aim to bridge the aforementioned gap by introducing a tractable mathematical framework, facilitating the derivation of analytical expressions

This work received funding from the European Research Council (ERC) under the European Union's Horizon 2020 research and innovation programme (Grant agreement No. 819819). It was also funded by the European Union's Horizon Europe programme (ERC, WAVE, Grant agreement No. 101112697), and from the European Union HORIZON programme under iSEE-6G GA No. 101139291.

for the ID and EH outage probability of FA-enabled SWIPT communication networks. The developed framework takes into account the employment of a power splitting (PS) scheme by the UEs to simultaneously extract information and harvest energy from the received RF signals, while a non-linear EH model is considered. Moreover, under specific practical assumptions, closed-form expressions for the Laplace transform of the received interference are derived. These closed-form expressions provide a quick and convenient methodology of evaluating the system's performance and obtaining insights into how key parameters affect the performance. Finally, our results highlight the beneficial synergy of FA technology and SWIPT systems, providing an increase of the achieved ID performance by around 30% compared with the conventional FAS-enabled communications, at the cost of a minor reduction of the EH performance by around 6%.

II. System Model

A. Network topology

Consider a downlink cellular network, where the locations of the randomly deployed base stations (BSs) are modeled as points of a homogeneous Poisson point process (PPP), denoted as $\Phi = \left\{x_j \in \mathbb{R}^2, j \in \mathbb{N}\right\}$ with density λ_b. To simplify the notation, we assume that the BSs' locations are ordered with respect to their distances from the origin. Hence, x_j represents the j-th closest BS to the origin with distance that is denoted as r_j i.e., $r_j = \|x_j\|$. Regarding the spatial deployment of UEs, we assume that their locations follow an arbitrary independent point process Ψ with density $\lambda_u \gg \lambda_b$. Due to the possible coexistence of multiple UEs within the coverage area of a BS, a scheduling mechanism is adopted, which schedules all UEs for their communication with the assigned BS at different time-frequency resources. Consequently, intra-cell UEs are served with orthogonal time-frequency resources, and thus, no intra-cell interference exists. A distance-based association rule is considered i.e., the typical UE at the origin communicates with its closest BS located at $x_0 \in \mathbb{R}^2$, referred as *tagged BS*, and its link with the typical UE is denoted as *typical link*[1]. Hence, the random variable (RV) representing the distance between the typical UE and the tagged BS follows a probability density function (pdf), that is given by [13]

$$f_R(r) = 2\pi\lambda_b r \exp(-\pi\lambda_b r^2). \tag{1}$$

Finally, we assume that all BSs are equipped with a single omnidirectional antenna, while all UEs are equipped with a single FA (see Section II-B).

B. Fluid antenna model

The concept of FA refers to a tube-like linear micro-channel or capillary filled with an electrolyte, containing of a drop of liquid metal (e.g., EGaIn) that can move freely within the capillary. The position of the fluid metal, referred as the antenna's location, can be promptly switched to one of N preset locations (also known as "ports"). These ports are evenly distributed along the linear dimension of the antenna, which is given by $\kappa\lambda$, where λ is the wavelength, and κ is a scaling constant. The distance of the link between the i-th port of the typical UE and the BS at $x_j \in \mathbb{R}^2$, is given by [8]

$$\rho_i(r_j) = \sqrt{r_j^2 + \left(\frac{\kappa\lambda d(i)}{N-1}\right)^2}, \ \forall\ i \in \mathcal{N}, \tag{2}$$

where r_j is the distance between the typical UE and the BS at $x_j \in \mathbb{R}^2$ i.e., $r_j = \|x_j\|$, and $d(i) = \frac{N+1}{2} - i$ if N is even, otherwise $d(i) = \lceil \frac{N}{2} - i \rceil$. Note that, the adopted FA model captures the conventional (i.e., static) omnidirectional antenna for the case where $N = 1$, enabling the evaluation of the performance achieved by the conventional communication networks, where UEs are equipped with FPAs.

C. Channel model

All wireless signals are subject to large-scale path-loss effects as well as small-scale fading. In particular, we consider that the large-scale attenuation incurred at the transmitted signals follows a general power-law model i.e., $\ell(r) = r^{-a}$, which assumes that the received power decays with the distance r between the transmitter located at X and the receiver located at Y i.e., $r = \|X - Y\|$, where $a > 2$ denotes the path-loss exponent. Regarding the small-scale fading, we assume that the fading channel coefficients between the i-th port of the typical UE and the BS at $x_j \in \mathbb{R}^2$, $|h_{i,j}|$, follow the Nakagami-μ distribution, and hence, the power gain of the channel fading is a normalized Gamma RV with shape parameter μ and scale parameter $1/\mu$ i.e., $|h_{i,j}|^2 \sim \Gamma[\mu, 1/\mu]$. Such general model will enable to consider a wide range of multi-path fading conditions, such as severe fading channels (Rayleigh fading when $\mu = 1$) and no fading channels (when $\mu \to \infty$), maintaining the tractability of the proposed mathematical framework. Due to the capability of the FAs' ports to be arbitrarily close to each other, the channel coefficients $|h_{i,j}|$ for $i \in \{1, 2, \ldots, N\}$ and $j \in \mathbb{N}$ are considered to be correlated [5]. Furthermore, we assume all wireless links exhibit additive white Gaussian noise with zero mean and variance σ^2.

D. Joint wireless information and power transfer model

We assume that all BSs have a continuous power supply and transmit with power P (dBm). In contrast, all UEs are assumed to be batteryless and capable of simultaneously decoding information and harvesting energy through a power-splitting SWIPT technique. Specifically, the received power is divided into two parts with a splitting ratio $\chi \in [0, 1]$, where a fraction $(1-\chi)$ of the received power is consumed for the ID purpose, while the remaining power is driven to the EH circuit [12].

Regarding the EH process, a UE harvests energy from the aggregate RF signal transmitted by all BSs. A practical EH model is adopted, which captures the randomness in the detection of the actual harvested energy [12]. Specifically, the harvested energy of a UE at the i-th port is equal to [12]

$$\psi_i = \frac{\chi\nu\eta}{1+F} \sum\nolimits_{\substack{j\in\mathbb{N} \\ x_j\in\Phi}} P|h_{i,j}|^2 \ell\left(\rho_i(r_j)\right), \tag{3}$$

where F is an exponential RV with mean ζ, $\nu = \zeta e^{\zeta} \int_{-\zeta}^{\infty} e^{-t}/t \mathrm{d}t$, and η is a constant representing the energy conversion efficiency from RF to direct current power.

[1]The adopted distance-based association policy requires an a priori knowledge of the location of the BSs. This knowledge can be obtained by monitoring the location of the BSs through a low-rate feedback channel or by a global positioning system mechanism.

E. Preliminary knowledge on copula theory

In order to acquire both analytical and closed-form expressions for the investigated performance metrics obtained in the considered network deployments under arbitrary correlated fading coefficients, we now briefly review some basic definitions and properties of the n- dimensional Copula [14].

Definition 1 (n-dimensional Copula)**.** *Let $\mathbf{V} = \{V_1, \ldots, V_n\}$ be a vector of n RVs with marginal cumulative distribution functions (cdfs) $F_{V_i}(v_i)$ for $i \in \{1, \ldots, n\}$, respectively. The corresponding joint cdf can be expressed as follows*

$$F_{V_1,\ldots,V_n}(v_1, \ldots, v_n) = \mathbb{P}[V_1 < v_1, \ldots, V_n < v_n]. \quad (4)$$

Then, the Copula function $C(v_1, \ldots, v_n)$ of the random vector $\mathbf{V}$ defined on the unit hypercube $[0, 1]^d$ with uniformly distributed RVs $V_i = F_{V_i}(v_i)$ for $i \in \{1, \ldots, n\}$ over $[0, 1]$ is given by

$$C(v_1, \ldots, v_n) = \mathbb{P}[V_1 < v_1, \ldots, V_n < v_n]. \quad (5)$$

In the literature, there is a plethora of well-known copula families [14]. The basis for the theory of copulas stems from the Sklar's theorem, which is stated in the following theorem.

Theorem 1 (Sklar's Theorem)**.** *Let $F_{V_1,\ldots,V_n}(v_1, \ldots, v_n)$ be a joint cdf of RVs with marginals $F_{V_i}(v_i)$ for $i \in \{1, \ldots, n\}$. Then, there exists one Copula function $C(v_1, \ldots, v_n)$ such that for all v_i in the extended real line domain $\mathbb{R}$,*

$$F_{V_1,\ldots,V_n}(v_1, \ldots, v_n) = C(F_{V_1}(v_1), \ldots, F_{V_n}(v_n)) \quad (6)$$

Although many types of copulas have been defined (e.g., Gaussian, Gumbel, etc), we exploit the Frank copula function [14] to analyze the performance metrics of the considered communication systems, which is defined in the following.

Definition 2 (Frank copula)**.** *The generalized Frank copula of n-dimension is defined as*

$$C(v_1, \ldots, v_n) = -\frac{1}{\beta} \ln\left(1 + \frac{\prod_{i=1}^{n} \left(\exp\left(-\beta v_i\right) - 1\right)}{\exp\left(-\beta\right) - 1}\right), \quad (7)$$

where $\beta \in \mathbb{R}\backslash\{0\}$ is the dependence parameter, which measures the dependence between the marginals. Thus, the special case $\beta \to 0$ captures the scenario where the marginals are independent between each other.

III. SWIPT in FA-enabled Systems

In this section, we assess the overall system performance in terms of EH and ID performance. We first evaluate the statistic properties of the aggregate interference, where analytical and closed-form expressions for the Laplace transform of the interference function are derived. Thereafter, analytical expressions for both ID and EH outage performance are derived, by using tools from SG and CT.

A. Interference Characterization

The aggregate interference at the i-th port of the typical UE can be expressed as follows

$$I^{(i)} = \sum_{\substack{j \in \mathbb{N} \\ x_j \in \Phi \backslash \{x_0\}}} I_j^{(i)} = \sum_{\substack{j \in \mathbb{N} \\ x_j \in \Phi \backslash \{x_0\}}} |h_{i,j}|^2 \ell\left(\rho_i(r_j)\right), \quad (8)$$

where $I_j^{(i)}$ represents the interference observed at the i-th port of the typical UE that is caused by the BS at $x_j \in \mathbb{R}^2$, $h_{i,j}$ and $\rho_i(r_j)$ are the channel fading and distance between the i-th port of the typical UE and the interfering BS at $x_j \in \mathbb{R}^2$, respectively. To characterize the interference, in the following lemma, we compute the Laplace transform of $I^{(i)}$ at s conditioned on r_0, which we denote as $\mathcal{L}_I(s)$.

Lemma 1. *The Laplace transform of the interference function, $\mathcal{L}_I(s)$, is given by*

$$\mathcal{L}_I(s) = \exp\left[-2\pi\lambda_b \int_{r_0}^{\infty} \left(1 - \left(1 + \frac{s}{\rho_i(r)^a}\right)^{-\mu}\right) r \mathrm{d}r\right], \quad (9)$$

where $\rho_i(r)$ represents the distance between the i-th port of the typical UE and the interfering BSs, that is given by (2)*.*

Proof. See Appendix A. □

By approximating the distance between any FA port of the typical UE and an interfering BS at $x_j \in \mathbb{R}^2$ with the distance between the origin and that particular interfering BS i.e., $\rho_i(r_j) \approx r_j$ for all $i \in \{1, 2, \ldots, N\}$, a closed-form expression for the Laplace transform of the interference function can be derived. This assumption is based on the fact that the distances between the FA ports are significantly smaller compared to the length of a link i.e., $r_j \gg \frac{\kappa\lambda}{2} \frac{1}{N-1}$, and therefore, inducing a negligible effect on the large-scale path loss. The following lemma provides a closed-form expression for $\mathcal{L}_I(s)$, based on the above observation and by letting $a = 4$.

Lemma 2. *With $a = 4$, the Laplace transform of the interference function, $\mathcal{L}_I(s)$, can be approximated as follows*

$$\mathcal{L}_I(s) \simeq \exp\left[\pi\lambda r_0^2 \left(1 - {}_2F_1\left[-\frac{1}{2}, \mu, \frac{1}{2}, -\frac{s}{r_0^4}\right]\right)\right], \quad (10)$$

where ${}_2F_1[\cdot, \cdot, \cdot, \cdot]$ is the hypergeometric function.

Proof. By substituting the expression $\rho_i(r_j) \approx r_j$ in (9), and by letting $a = 4$, the final expression can be derived. □

To gain more insights on the performance of the considered network deployments, we also focus on a use-case of practical interest. In particular, we consider the case where all links experience Rayleigh fading, i.e. $\mu = 1$, capturing the scenario where the UEs experience weak and/or obstructed line-of-sight communication links. The analytical expression for the Laplace transform of the interference function under the Rayleigh fading scenario, denoted as $\widetilde{\mathcal{L}}_I(s)$, is provided in the following Lemma.

Lemma 3. *With Rayleigh fading and $a = 4$, the Laplace transform of the interference function, $\widetilde{\mathcal{L}}_I(s)$, is given by*

$$\widetilde{\mathcal{L}}_I(s) = \exp\left[-\frac{\pi\lambda\sqrt{s}}{2}\left(\pi - 2\arctan\left[\frac{\rho_0(r_0)^2}{\sqrt{s}}\right]\right)\right], \quad (11)$$

where $\arctan[\cdot]$ is the inverse tangent function and $\rho_0(r_0)$ is the distance of the link between the i-th port of the typical UE and the tagged BS at $x_0 \in \mathbb{R}^2$, that is given by (2)*.*

Proof. By substituting $\mu = 1$ in (9), $\mathcal{L}_I(s)$ can be written as

$$\widetilde{\mathcal{L}}_I(s) = \exp\left[-2\pi\lambda \int_{r_0}^{\infty} \frac{s\rho_i(r)^{-a+1}}{1 + s\rho_i(r)^{-a}} \mathrm{d}r\right]. \quad (12)$$

Then, by setting $a = 4$, the final expression can be derived. □

B. Port Selection Scheme

For the successful operation of both ID and EH process of each UE, it is required to adopt a port selection scheme in order to determine the location of its FA location. We assume that the FA's location of each UE is switched to the port that experience the maximum signal-to-interference ratio (SIR). The adopted max-SIR port selection scheme ensures the best reception performance by exploiting the additional degrees of freedom offered by the FA technology via selecting a port that ensures suppressed inter-cell interference without complex signal processing techniques. Hence, the FA's location of each UE is instantly switched to the port that satisfies

$$\mathtt{i} = \arg\max_{i\in\mathcal{N}} \left\{ \frac{|h_{i,0}|^2 \ell(\rho_i(r_0))}{\sum\limits_{\substack{j\in\mathbb{N} \\ x_j\in\Phi\setminus\{x_0\}}} |h_{i,j}|^2 \ell\left(\rho_i(r_j)\right)} \right\}. \quad (13)$$

Let ω_i represents the observed SIR at the i-th port i.e., $\omega_i = |h_{i,0}|^2\ell(\rho_i(r_0))/\sum\limits_{\substack{j\in\mathbb{N} \\ x_j\in\Phi\setminus\{x_0\}}} |h_{i,j}|^2\ell\left(\rho_i(r_j)\right)$ and the RV Ω depicts the maximum SIR observed at the selected port $\mathtt{i}$ i.e., $\Omega = \max_{i\in\mathcal{N}}\{\omega_1,\omega_2,\ldots,\omega_N\}$. Then, the conditional cdf of Ω i.e., $F_\omega(\theta|r_0)$, in the context of Frank copula is mathematically derived in the following Lemma.

Lemma 4. *The cdf of $\Omega = \max_{i\in\mathcal{N}}\{\omega_1,\omega_2,\ldots,\omega_N\}$ is given by*

$$F_\Omega(\theta|r_0) = -\frac{1}{\beta}\ln\left(1+\frac{\left(\exp\left[-\beta F_\omega(\theta|r_0)\right]-1\right)^N}{\exp\left[-\beta\right]-1}\right), \quad (14)$$

where

$$F_\omega(\theta|r_0) = \sum_{k=1}^{\mu}(-1)^{k+1}\binom{\mu}{k}\mathcal{L}_I\left(\frac{\xi k\theta}{\ell(\rho_i(r_0))}\right), \quad (15)$$

$\xi = \mu(\mu!)^{-\frac{1}{\mu}}$ and $\mathcal{L}_I(\cdot)$ represents the Laplace transform of $I^{(i)}$, that is given in Lemma 1.

Proof. See Appendix B. □

C. Information transfer performance

We investigate the achieved ID outage probability of a FA-enabled UE in the context of large-scale cellular networks, that can be defined as the probability of unsuccessfully decoding the desired signal by the selected port of the typical UE. The above-mentioned performance metric can be mathematically described with the probability $\mathbb{P}\left[\frac{|h_{\mathtt{i},0}|^2\ell(\rho_{\mathtt{i}}(r_0))}{I^{(\mathtt{i})}+\sigma^2} < \theta_{\mathrm{I}}\right]$. An analytical expression for the instantaneous outage probability is provided in the following Theorem.

Theorem 2. *The ID outage probability in the context of FA-enabled SWIPT cellular networks, is given by*

$$\Pi^{\mathrm{ID}}(\theta_{\mathrm{I}}) = \int_0^\infty F_\Omega(\theta_{\mathrm{I}}|r_0)\exp\left(-\frac{\theta_{\mathrm{I}}\sigma^2}{(1-\chi)P\mathbb{E}I}\right)f_R(r_0)\mathrm{d}r_0, \quad (16)$$

where $\beta\in\mathbb{R}\backslash\{0\}$, $F_\Omega(\cdot|r_0)$ depicts the conditional cdf of the correlated SIR observed at the FA's ports, that is assessed in Lemma 4, $\mathbb{E}I$ is the mean of the aggregate interference at the selected FA port and is equal to

$$\mathbb{E}I = \frac{2\pi\lambda_b}{a-2}\ell(\rho_{\mathtt{i}}(r_0))^2, \quad (17)$$

and $f_R(r_0)$ is the pdf of the distance between the typical UE and the tagged BS, that is given by (1)*.*

Proof. See Appendix C □

Under the assumption of Rayleigh fading and $a = 4$, an analytical expression for the achieved ID outage probability in the context of the considered network deployments is provided in the following Proposition.

Proposition 1. *With Rayleigh fading and $a = 4$, the ID outage probability in the context of FA-enabled SWIPT cellular networks, is given by*

$$\widetilde{\Pi}^{\mathrm{ID}}(\theta_{\mathrm{I}}) = \int_0^\infty \ln\left[1+\frac{\left(\exp\left[-\beta\widetilde{\mathcal{L}}_I\left(\frac{\theta_{\mathrm{I}}}{\ell(\rho_i(r_0))}\right)\right]-1\right)^N}{\exp\left[-\beta\right]-1}\right]^{-\frac{1}{\beta}} \times \exp\left(-\frac{\theta_{\mathrm{I}}\sigma^2}{(1-\chi)P\mathbb{E}I}\right)2\pi\lambda_b r_0\exp(-\pi\lambda_b r_0^2)\mathrm{d}r_0, \quad (18)$$

where $\beta\in\mathbb{R}\backslash\{0\}$, $\widetilde{\mathcal{L}}_I(\cdot)$ depicts the Laplace transform of the interference under the assumption of Rayleigh fading and $a = 4$, that is evaluated in Lemma 3.

Proof. The proof follows similar methodology as described in Appendix C, but using the expression obtained in Lemma 3 and setting $\mu = 1$, and thus, is omitted for brevity. □

D. Energy harvesting performance

We investigate the EH performance, that is mathematically defined as the probability that the instantaneous harvested energy, denoted as $\psi_{\mathtt{i}}$, is smaller than a predefined threshold θ, and is expressed as $\Pi^{\mathrm{EH}}(\theta) = \mathbb{P}[\psi_{\mathtt{i}} < \theta_{\mathrm{E}}]$. This metric provides valuable insights into the effectiveness of an EH-enabled system, as it enables us to quantify the probability that a given level of energy can be reliably harvested. An analytical expression for the EH outage probability is provided in the following theorem.

Theorem 3. *The EH outage probability of the typical UE is given by*

$$\Pi^{\mathrm{EH}}(\theta_{\mathrm{E}}) = \int_0^\infty F_\Omega\left(\vartheta|r_0\right)f_R(r_0)\mathrm{d}r_0, \quad (10)$$

where $\beta\in\mathbb{R}\backslash\{0\}$, $\vartheta = \frac{\theta_{\mathrm{E}}(1+F)}{\chi\nu\eta P\mathbb{E}I} - 1$, $F_\Omega(\cdot|r_0)$ is the conditional cdf of the correlated SIR observed at the FA's ports, that is given in Lemma 4, and $f_R(r_0)$ is given by (1)*.*

Proof. See Appendix D. □

Regarding the scenario where all links experience Rayleigh fading and the path-loss exponent is equal to $a = 4$, the following Proposition presents an analytical expression for the achieved EH outage probability in the context of the considered network deployments.

Proposition 2. *With Rayleigh fading and $a = 4$, the EH outage probability in the context of FA-enabled SWIPT cellular networks, is given by*

$$\widetilde{\Pi}^{\mathrm{EH}}(\theta_{\mathrm{E}}) = \int_0^\infty \ln\left[1+\frac{\left(\exp\left[-\beta\widetilde{\mathcal{L}}_I\left(\frac{\vartheta}{\ell(\rho_i(r_0))}\right)\right]-1\right)^N}{\exp[-\beta]-1}\right]^{-\frac{1}{\beta}} \times 2\pi\lambda_b r_0\exp(-\pi\lambda_b r_0^2)\mathrm{d}r_0, \quad (11)$$

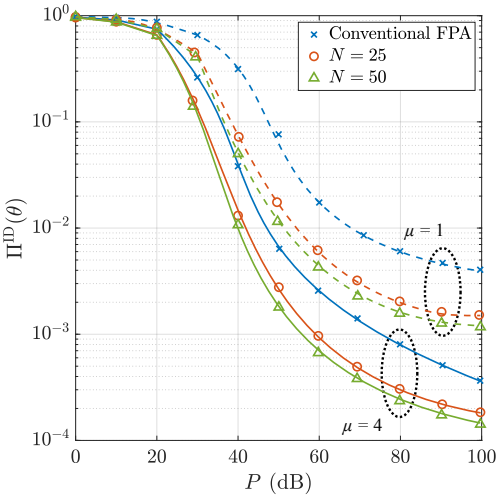

Fig. 1: ID outage performance versus the threshold θ (dB) under both Nakagami and Rayleigh channel fading for different number of ports N.

where $\beta \in \mathbb{R}\backslash\{0\}$, $\vartheta = \frac{\theta_{\mathrm{E}}(1+F)}{\chi\nu\eta P\mathbb{E}I} - 1$, $\mathbb{E}I$ *represents the mean interference, that is given by* (17), $\widetilde{\mathcal{L}}_I(\cdot)$ *depicts the Laplace transform of the interference under the assumption of Rayleigh fading and* $a = 4$*, that is evaluated in Lemma 3.*

IV. Numerical Results

We provide numerical results to verify our model and to demonstrate the performance of FA-enabled UEs in large-scale SWIPT systems. Specifically, we consider the following parameters: $\lambda_b = 15\mathrm{BS/km}^2$, $\lambda_u = 30\mathrm{BS/km}^2$, $\lambda = 6$ cm, $W = 500$ kHz, $\kappa = 0.2$, $a = 4$, $\sigma = 1$, $\chi = 0.5$, and $\zeta = 0.01$. Note that, different values will lead to a shifted network performance, but with the same conclusions. The lines (dashed or solid) and markers in the plots represent the analytical and simulation results, respectively.

In Fig. 1, the ID performance of FA-enabled UEs over Nakagami fading is illustrated in the context of large-scale SWIPT cellular networks versus the transmit power P (dB). For comparison purposes, the network performance over Rayleigh fading is also displayed in the figure as a dashed line. The first main observation is that the performance under Nakagami channel fading outperforms that achieved under Rayleigh channel fading. This observation can be explained by the fact that by increasing the quality of the communication link, UEs experience lower fading over their received signal, thus the network performance increases. Furthermore, the increased number of FA ports leads to the enhanced ID performance. This was expected, since by increasing the number of FA ports, the spatial diversity also enhances, resulting in an elevated SIR observed by the UEs. Moreover, in comparison to the performance achieved by UEs that are equipped with a conventional FPA, denoted as "Conventional FPA", FA-enabled SWIPT systems achieve better network performance. Finally, the ID performance improves with P and as P increases, it converges to a lower bound.

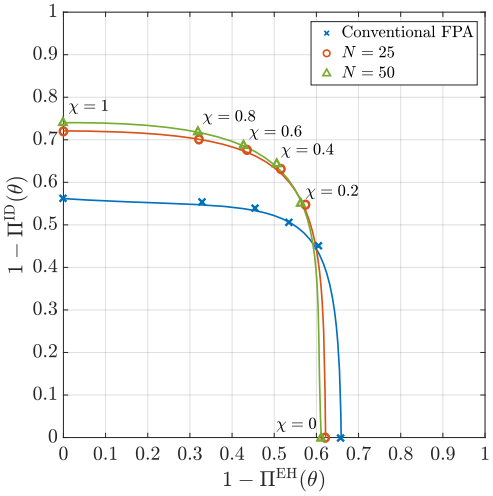

Fig. 2: Trade-off between the ID and EH performance for different PS fractions χ.

Fig. 2 shows the feasibility region of the FA-enabled SWIPT systems with respect to the PS parameter. More specifically, each point in the curves represents the trade-off between the ID coverage performance (i.e., $1 - \Pi^{\mathrm{ID}}(\theta)$) and EH coverage performance (i.e., $1 - \Pi^{\mathrm{EH}}(\theta)$) for a given PS ratio χ. For comparison purposes, the performance achieved by UEs that are equipped with a conventional FPA is also displayed, denoted as "Conventional FPA". The main observation is that, although the employment of FA at the UEs leads to a minor decrease in the EH performance by around 6%, the achieved ID performance is significantly enhanced by around 30%. This was expected, since the elevated number of FA ports enables the selection of a port that observes less multi-user interference, and therefore the achieved SIR becomes larger while the total harvested energy decreases.

V. Conclusion

For the purpose of addressing the new and inevitable challenges on modeling and analysing the correlated fading channels of large-scale FA-enabled systems, in this paper, we have explored the synergy of SG and CT. We initially derived a closed-form expression for the cdf of the observed SIR under correlated Nakagami-m fading in the context of CT. According to the CT-based approach, a SG-based framework has been presented, where analytical expressions for the SWIPT performance of the considered network deployments have been derived, by taking into account the employment of a PS scheme by the UEs, as well as a non-linear EH model. Our results show that the synergy of CT and SG is a promising solution to overcome the difficulties imposed by the FA technology in modeling and analysis of large-scale FA-enabled SWIPT cellular networks. Finally, we have shown that the FA technology provides an increase of around 30% in terms of ID performance at the cost of a minor reduction of the EH performance by 6%, compared to that achieved by the conventional FPA systems.

APPENDIX A
PROOF OF LEMMA 1

The Laplace transform definition yields

$$\mathcal{L}_I(s) = \mathbb{E}_{\Phi,h_i}\left[\prod_{\substack{j\in\mathbb{N}\\ x_j\in\Phi\setminus\{x_0\}}} \exp\left[-s|h_{i,j}|^2\ell\left(\rho_i(r_j)\right)\right]\right].$$

By using SG tools, and specifically the probability generating functional of a PPP [13], we can analytically represent the Laplace transform of $I^{(i)}$ as follow

$$\mathcal{L}_I(s)$$
$$=\exp\left[-2\pi\lambda\int_{r_0}^{\infty}\left(1-\mathbb{E}_{h_{i,j}}\left[\exp\left[-s|h_{i,j}|^2\ell\left(\rho_i(r_j)\right)\right]\right]\right)r\mathrm{d}r\right],$$

where $\mathbb{E}_{h_{i,j}}\left[\exp\left[-x|h_{i,j}|^2\right]\right]$ corresponds to the moment generating function (MGF) of the gamma RV $|h_{i,j}|^2$ with integer parameter μ, and is given by $(1+x)^{-\mu}$. Thus, the final expression in Lemma 1 can be derived.

APPENDIX B
PROOF OF LEMMA 4

Based on the definition, $F_\Omega(\theta|r_0)$ can be defined as

$$\begin{aligned}F_\Omega(\theta|r_0) &= \mathbb{P}\left[\max_{i\in\mathcal{N}}\{\omega_1,\omega_2,\ldots,\omega_N\}\le\theta|r_0\right]\\ &= F_{\omega_1,\omega_2,\ldots,\omega_N}(\theta,\theta,\ldots,\theta|r_0)\\ &= C(F_{\omega_1}(\theta|r_0),F_{\omega_2}(\theta|r_0),\ldots,F_{\omega_N}(\theta|r_0)),\end{aligned} \quad (12)$$

where (12) is derived from Theorem 1, and $F_{\omega_i}(\theta)$ represents the cdf of the observed SIR at the i-th port of the typical UE. The marginal distributions of ω_i is given by

$$F_{\omega_i}(\theta|r_0) = \mathbb{P}\left[|h_{i,0}|^2 \le \frac{\theta I^{(i)}}{\ell(\rho_i(r_0))}\middle| r_0\right], \quad (13)$$

where $|h_{i,0}|^2$ is a gamma distributed RV with parameter μ. To overcome the difficulty on Nakagami fading, Alzer's Lemma [13] on the cdf of a gamma RV with integer parameter can be applied. This relates the cdf of a gamma RV into a weighted sum of the cdfs of exponential RVs. Hence, we can bound expression (13) as

$$\begin{aligned}F_{\omega_i}(\theta|r_0) &< \mathbb{E}_{I^{(i)}}\left[\left(1-\exp\left[-\frac{\xi\theta I^{(i)}}{\ell(\rho_i(r_0))}\right]\right)^{\mu}\middle| r_0\right]\\ &= \sum_{k=1}^{\mu}(-1)^{k+1}\binom{\mu}{k}\mathbb{E}_{I^{(i)}}\left[\exp\left[-\frac{\xi k\theta I^{(i)}}{\ell(\rho_i(r_0))}\right]\middle| r_0\right],\end{aligned} \quad (14)$$

where (14) is derived with the use of Alzer's Lemma [13] and $\xi = \mu(\mu!)^{-\frac{1}{\mu}}$. Note that the expectation in (14) is the Laplace transform of the interference function, $\mathcal{L}_I(s)$ where $s = \frac{\xi k\vartheta}{\ell(\rho_i(r_0))}$. Then, by setting $F_\omega(\theta) = F_{\omega_i}(\theta)\ \forall i\in\mathcal{N}$ and by substituting the derived expression in (12), the final expression in Lemma 4 can be derived.

APPENDIX C
PROOF OF THEOREM 2

The ID outage performance can be calculated as follows

$$\Pi^{\mathrm{ID}}(\theta) = \mathbb{P}\left[\frac{|h_{\mathtt{i},0}|^2\ell\left(\rho_{\mathtt{i}}(r_0)\right)}{I^{(\mathtt{i})}+\frac{\sigma^2}{(1-\chi)P}} < \theta\right],$$

where by approximating the aggregate network interference with its mean and by un-conditioning the derived expression with the pdf of the distance from the typical UE to its serving BS i.e., $f_R(r_0)$, the final expression can be derived.

APPENDIX D
PROOF OF THEOREM 3

Based on the definition, $\Pi^{\mathrm{EH}}(\theta)$ can be defined as

$$\Pi^{\mathrm{EH}}(\theta) = \mathbb{P}\left[\frac{\chi\nu\eta}{1+F}\sum_{\substack{j\in\mathbb{N}\\ x_j\in\Phi}} P|h_{\mathtt{i},j}|^2\ell\left(\rho_{\mathtt{i}}(r_j)\right)\le\theta\right]$$

$$\approx\mathbb{P}\left[\frac{|h_{\mathtt{i},0}|^2\ell\left(\rho_{\mathtt{i}}(r_0)\right)}{\sum\limits_{\substack{j\in\mathbb{N}\\ x_j\in\Phi\setminus\{x_0\}}}|h_{\mathtt{i},j}|^2\ell\left(\rho_{\mathtt{i}}(r_j)\right)}\le\frac{\theta(1+F)}{\chi\nu\eta P\mathbb{E}I}-1\right], \quad (15)$$

where (15) is derive by approximating the power of the aggregate interference signals at the $\mathtt{i}$-th port of the typical UE with its mean i.e., $I^{(n)}\approx\mathbb{E}I=\frac{2\pi\lambda_b}{a-2}\ell(\rho_{\mathtt{i}}(r_0))^2$ [13]. Then, by following similar steps as in Appendix B, the EH outage performance can be re-written as $\Pi^{\mathrm{EH}}(\theta)=\mathbb{E}_{r_0}\left[F_\Omega\left(\vartheta|r_0\right)\right]$, where $\vartheta=\frac{\theta(1+F)}{\chi\nu\eta P\mathbb{E}I}-1$, $F_\Omega(\cdot|r_0)$ is the conditional cdf of the correlated SIR observed at the FAs' ports, that is evaluated in Lemma 4. Thus, the final expression can be derived by un-conditioning the above expression with the pdf of the distance from the typical UE to its serving BS i.e., $f_R(r_0)$.

REFERENCES

[1] I. F. Akyildiz, A. Kak, and S. Nie, "6G and beyond: The future of wireless communications systems," *IEEE Access,* vol. 8, pp. 133995–134030, 2020.

[2] A. F. Molisch, V. V. Ratnam, S. Han, Z. Li, S. L. H. Nguyen, L. Li, and K. Haneda, "Hybrid beamforming for massive MIMO: A survey," *IEEE Commun. Mag.*, vol. 55, no. 9, pp. 134–141, Sep. 2017.

[3] Y. Huang, L. Xing, C. Song, S. Wang, and F. Elhouni, "Liquid antennas: Past, present and future," *IEEE Open J. Antennas Propag.,* vol. 2, pp. 473–487, 2021.

[4] L. Zhu, W. Ma, and R. Zhang, "Movable-antenna array enhanced beamforming: Achieving full array gain with null steering," *arXiv preprint arXiv:2308.08787*, 2023.

[5] K. K. Wong and K. F. Tong, "Fluid antenna multiple access," *IEEE Trans. Wireless Commun.,* vol. 21, no. 7, pp. 4801–4815, Jul. 2022.

[6] M. Khammassi, A. Kammoun, and M.-S. Alouini, "A new analytical approximation of the fluid antenna system channel," *arXiv preprint arXiv:2203.09318*, 2023.

[7] C. Skouroumounis and I. Krikidis, "Fluid antenna-aided full duplex communications: A macroscopic point-of-view," *arXiv preprint arXiv:2304.04435*, 2023.

[8] C. Skouroumounis and I. Krikidis, "Fluid antenna with linear MMSE channel estimation for large-scale cellular networks," *IEEE Trans. Commun.,* vol. 71, no. 2, pp. 1112–1125, Feb. 2023.

[9] F. R. Ghadi, K.-K. Wong, F. J. Lopez-Martınez, C.-B. Chae, K.-F. Tong, and Y. Zhang "A Gaussian copula approach to the performance analysis of fluid antenna systems," *arXiv preprint arXiv:2309.07506*, 2023.

[10] I. Krikidis, S. Timotheou, S. Nikolaou, G. Zheng, D. W. K. Ng, and R. Schober, "Simultaneous wireless information and power transfer in modern communication systems," *IEEE Commun. Mag.,* vol. 52, no. 11, pp. 104–110, Nov. 2014.

[11] M. Di Renzo and W. Lu, "System-level analysis and optimization of cellular networks with simultaneous wireless information and power transfer: Stochastic geometry modeling," *IEEE Trans. Veh. Technol.,* vol. 66, no. 3, pp. 2251–2275, Mar. 2017.

[12] N. Deng and M. Haenggi, "The energy and rate meta distributions in wirelessly powered D2D networks," *IEEE J. Sel. Areas Commun.,* vol. 37, no. 2, pp. 269–282, Sep. 2019.

[13] M. Haenggi, *Stochastic geometry for wireless networks*, in *Cambridge*, U.K.: Cambridge Univ. Press, 2012.

[14] R. B. Nelsen, *An introduction to copulas*, in *Springer science & business media*, 2007.